doi:10.1093/brain/awu007 Brain 2014: 137; 1039–1050 | 1039

BRAIN
A JOURNAL OF NEUROLOGY

Enhanced excitability of MRGPRA3- and MRGPRD-positive nociceptors in a model of inflammatory itch and pain

Lintao Qu,[1,*] Ni Fan,[1,2,*] Chao Ma,[1,3] Tao Wang,[1,3] Liang Han,[4] Kai Fu,[1] Yingdi Wang,[5] Steven G. Shimada,[1] Xinzhong Dong[4] and Robert H. LaMotte[1]

1 Department of Anaesthesiology, Yale University School of Medicine, New Haven, CT, 06520, USA
2 Guangzhou Brain Hospital, the Affiliated Hospital of Guangzhou Medical University, Guangzhou, Guangdong, China 510370
3 Institute of Basic Medical Sciences, Chinese Academy of Medical Sciences, School of Basic Medicine, Peking Union Medical College, Department of Anatomy, Histology and Embryology, Beijing, China
4 Department of Neuroscience, Johns Hopkins University School of Medicine, Baltimore, MD, 21205, USA
5 Section of Cardiovascular Medicine, Department of Internal Medicine, Yale University School of Medicine, New Haven, CT 06511, USA

*These authors contributed equally to this work.

Correspondence to: Robert H. LaMotte, Ph.D.,
Department of Anaesthesiology, Yale University School of Medicine,
333 Cedar Street, New Haven, CT 06520, USA
E-mail: robert.lamotte@yale.edu

Itch is a common symptom of diseases of the skin but can also accompany diseases of other tissues including the nervous system. Acute itch from chemicals experimentally applied to the skin is initiated and maintained by action potential activity in a subset of nociceptive neurons. But whether these pruriceptive neurons are active or might become intrinsically more excitable under the pathological conditions that produce persistent itch and nociceptive sensations in humans is largely unexplored. Recently, two distinct types of cutaneous nociceptive dorsal root ganglion neurons were identified as responding to pruritic chemicals and playing a role in itch sensation. One expressed the mas-related G-coupled protein receptor MRGPRA3 and the other MRGPRD (MRGPRA3$^+$ and MRGPRD$^+$ neurons, respectively). Here we tested whether these two distinct pruriceptive nociceptors exhibited an enhanced excitability after the development of contact hypersensitivity, an animal model of allergic contact dermatitis, a common pruritic disorder in humans. The characteristics of increased excitability of pruriceptive neurons during this disorder may also pertain to the same types of neurons active in other pruritic diseases or pathologies that affect the nervous system and other tissues or organs. We found that challenging the skin of the calf of the hind paw or the cheek of previously sensitized mice with the hapten, squaric acid dibutyl ester, produced symptoms of contact hypersensitivity including an increase in skin thickness and site-directed spontaneous pain-like (licking or wiping) and itch-like (biting or scratching) behaviours. Ablation of MRGPRA3$^+$ neurons led to a significant reduction in spontaneous scratching of the hapten-challenged nape of the neck of previously sensitized mice. *In vivo*, electrophysiological recordings revealed that MRGPRA3$^+$ and MRGPRD$^+$ neurons innervating the hapten-challenged skin exhibited a greater incidence of spontaneous activity and/or abnormal after-discharges in response to mechanical and heat stimuli applied to their receptive fields compared with neurons from the vehicle-treated control animals. Whole-cell recordings *in vitro* showed that both MRGPRA3$^+$ and MRGPRD$^+$ neurons from hapten-challenged mice displayed a significantly more depolarized resting membrane potential, decreased rheobase, and greater number of action potentials at twice rheobase compared with neurons from vehicle controls. These signs of neuronal hyperexcitability were associated with a significant increase in the peak amplitude of tetrodotoxin-sensitive and resistant sodium currents. Thus, the hyperexcitability of MRGPRA3$^+$ and MRGPRD$^+$ neurons, brought about in part by enhanced sodium

Received August 12, 2013. Revised November 11, 2013. Accepted December 1, 2013. Advance Access publication February 18, 2014

currents, may contribute to the spontaneous itch- and pain-related behaviours accompanying contact hypersensitivity and/or other inflammatory diseases in humans.

Keywords: itch; pain; MRGPRA3; MRGPRD; allergic contact dermatitis

Abbreviations: CHS = contact hypersensitivity; GFP = green fluorescent protein; SADBE = squaric acid dibutyl ester; TTX = tetrodotoxin

Introduction

Itch is a fundamental sensory quality that is different from pain, but similar in its capacity to cause suffering and a decrease in the quality of life (Kini *et al.*, 2011; Chen, 2012). Recent evidence suggests that chemical stimuli that elicit acute itch in humans and animals evoke action potentials in a specific subset of cutaneous nociceptors. These nociceptors, termed 'pruriceptive' because they respond to a pruritic agent, also respond to one or more noxious stimuli (Schmelz *et al.*, 2003; Johanek *et al.*, 2008; Ringkamp *et al.*, 2011; Liu *et al.*, 2012; Han *et al.*, 2013). However, there is little information about whether activity in pruriceptive neurons might be abnormally generated during disorders that cause chronic itch. Neither is it known whether these neurons might become intrinsically hyperexcitable, thereby making them more responsive to endogenous stimuli normally present or pathologically generated. Our purpose here was to examine the changes in the excitability of pruriceptive neurons using a model of an inflammatory cutaneous disease, allergic contact dermatitis, which can be similarly produced in mice and humans (Scott *et al.*, 2002; Camouse *et al.*, 2008; Sikand *et al.*, 2012). It is anticipated that the characteristics of the enhanced excitability of pruriceptive neurons accompanying this disease may be of relevance to the chronic itch and/or pruritic and nociceptive dysaesthesias that can accompany injuries or disorders of the peripheral nerve or other tissues or organs.

In mice, two distinct types of dorsal root ganglion neurons each expressing a different mas-related G-protein-coupled receptor have been implicated in chemically-evoked itch (Liu *et al.*, 2012; Han *et al.*, 2013). One type of neuron expresses MRGPRA3, the receptor for the agonist, chloroquine, and the other type, MRGPRD, the receptor for the agonist beta-alanine (Shinohara *et al.*, 2004; Liu *et al.*, 2012). Each neuronal type has unmyelinated axons that exclusively innervate the stratum granulosum of the epidermis (Liu *et al.*, 2012; Han *et al.*, 2013). MRGPRA3$^+$ neurons are essential for normal histamine-dependent itch behaviour (Han *et al.*, 2013). There is evidence that MRGPRD$^+$ neurons contribute to mechanically evoked pain (Cavanaugh *et al.*, 2009) but also to the histamine-independent itch evoked by the MRGPRD receptor agonist beta alanine (Liu *et al.*, 2012). Though both types of nociceptors play a role in mediating itch evoked by acutely delivered pruritic stimuli, it is not known whether these neurons become more excitable in mice under a pathological condition that produces itch and nociceptive sensations in humans.

In the present study we examined the changes in the excitability of MRGPRA3$^+$ and MRGPRD$^+$ neurons innervating a cutaneous region of inflammation induced by a Type IV delayed contact hypersensitivity (CHS) reaction to an allergen to which the animal was previously sensitized—a model of allergic contact dermatitis. Preliminary results of this study were presented in abstract form (Fan *et al.*, 2012).

Materials and methods

Animals

The mice were C57BL/6 males, 2 to 3 months of age and weighing 20–30 g. Wild-type mice were used for behavioural testing. The donors for our colony of MRGPRA3 and MRGPRD transgenic mice were provided by Dr Xinzhong Dong's laboratory (John Hopkins University) and used for the electrophysiological recordings of cell bodies that expressed green fluorescent protein (GFP). For one type of mouse, the GFP was in neurons that expressed the MRGPRA3 receptor (MRGPRA3$^+$ neurons; Han *et al.*, 2013) whereas the other type of mouse exhibited the GFP in neurons that expressed the MRGPRD receptor (MRGPRD$^+$ neurons; Zylka *et al.*, 2005). MRGPRA3$^{GFP\text{-}Cre}$;ROSA26^{DTR} mice were generated as described (Han *et al.*, 2013). Briefly, the MRGPRA3$^{GFP\text{-}Cre}$ transgenic line was crossed with Cre-dependent ROSA26^{DTR} line, followed by diphtheria toxin (DTX; EMD Biosciences) injected intraperitoneally (40 μg/kg) twice, separated by 72 h (Han *et al.*, 2013). All the experimental procedures were approved by the Institutional Animal Care and Use Committee of Yale University School of Medicine (or for the use of MRGPRA3$^{GFP\text{-}Cre}$;ROSA26^{DTR} mice, Johns Hopkins University School of Medicine) and were in accordance with the guidelines provided by the National Institute of Health and the International Association for the Study of Pain.

Model of allergic contact dermatitis

The contact sensitizer squaric acid dibutylester (SADBE) (Tokyo Chemical Co.) was used to elicit CHS in the mouse as a model of allergic contact dermatitis in humans (Scott *et al.*, 2002; Camouse *et al.*, 2008; Sikand *et al.*, 2012). Mice were sensitized by the topical application of 25 μl of 1% SADBE in acetone (520 μg/cm^2) to the shaved abdominal skin once a day for three consecutive days (Scott *et al.*, 2002). Five days later, the SADBE-treated group was challenged with a topical application of 25 μl of 1% SADBE to the hairy skin of the foot and hind leg (for electrophysiology) or just onto the calf of one hind leg or, alternatively, to the right cheek (for behavioural testing) once a day for two consecutive days whereas acetone alone was used as the vehicle control. The thickness of calf skin was measured with a caliper before and 24 h after the second challenge as an assessment of inflammation. A similar protocol was used in a behavioural test using MRGPRA3$^{GFP\text{-}Cre}$;ROSA26^{DTR} mice to test the effects of ablating MRGPRA3$^+$ neurons on CHS-induced scratching. However, in this test, the mice were challenged on the nape of the neck with

0.5% of SADBE delivered once daily for four consecutive days before behavioural testing.

Behavioural testing

All behavioural tests of SADBE sensitized mice were performed just before administering the first challenge of SADBE ('pre-challenge' test) and then again 24 h after each SADBE challenge or application of acetone vehicle. Behavioural responses were video recorded by a camcorder. The video recording was subsequently played back offline in slow-motion to permit detailed measurements of behavioural responses directed toward the challenge site.

For the calf model, the duration of each biting or licking action directed toward the calf was timed by a stopwatch and summed to provide the cumulative biting or licking time over a period of 1 h as described (LaMotte *et al.*, 2011). Licking behaviour consisted of a series of long-stroke, bobbings of the head (~4 Hz) during which the tongue could sometimes be seen moving across the skin. Biting behaviour was characterized not by head movements, but by gnawing-like movements of the mandible (~15 Hz) (LaMotte *et al.*, 2011). For the nape of the neck model, scratching behaviour with the hind paw was quantified by recording the number of incidences of scratching bouts for 1 h (Liu *et al.*, 2009). For the cheek model, the number of bouts of spontaneous scratching with the hindpaw and wiping with the forepaw (Shimada and LaMotte, 2008) were counted for 2 h (a longer period of observation than for the calf or neck because of the fewer frequencies of spontaneous site-directed behaviours).

In vivo electrophysiological recordings

The properties of dorsal root ganglion neurons innervating the skin of the hind limb of mice were recorded *in vivo* using extracellular recording as described (Ma *et al.*, 2010, 2012). Briefly, under isoflurane anaesthesia, after laminectomy at the levels of L2–L6, the L3 dorsal root ganglion was fixed to a plate, and superfused with warm (~37°C) oxygenated artificial CSF at flow rate of 3 ml/min within a pool formed by a ring to which the skin was sewn. After removal of the epineurium, the neurons on the surface of the dorsal root ganglion were viewed by reflection microscopy and epifluorescence (to identify the presence of GFP indicative of MRGPRD$^+$ or MRGPRA3$^+$ expression).

Extracellular recordings were made on individual dorsal root ganglion neurons using a micropipette electrode with a tip of 20–25 μm. The sensory submodality of a neuron was classified according to its responses to chemical, heat and/or mechanical stimuli applied to its peripheral receptive field. These stimuli included innocuous stroking with a cotton-tipped probe, a gentle pinch using the experimenter's fingers and von Frey filaments with a fixed tip diameter (200 μm) but delivering different bending forces (for noxious mechanical stimuli), and a temperature-controlled chip-resistor heating probe (for noxious heat stimuli) (Ma *et al.*, 2010). The noxious heating stimulus had a trapezoidal temperature waveform with a ramp (1 s) from a base of 38°C to a plateau of 51°C (5 s) followed by a ramp back to the base. Conduction velocity was obtained by electrically stimulating the peripheral receptive field with two wire electrodes or sometimes a saline soaked cotton probe and calculated by dividing the latency of a spike peak by the distance between the stimulation electrode and the soma of the recorded neurons. The neuron was classified as spontaneously active only if spontaneous ongoing discharges occurred during a 3-min period without any external stimulation (Ma and LaMotte, 2007).

Acute culture of dorsal root ganglion neurons

The cell bodies of dorsal root ganglion neurons from adult MRGPRD$^+$ and MRGPRA3$^+$ mice were acutely dissociated as described (Qu *et al.*, 2012). Briefly, L3 and L4 lumbar dorsal root ganglions, ipsilateral to either acetone control or SADBE-treated skin, were harvested from mice 24 h after the second SADBE challenge or application of acetone vehicle and transferred into oxygenated complete saline solution for cleaning and mincing. The complete saline solution contained (mM): 137 NaCl, 5.3 KCl, 1 $MgCl_2$, 3 $CaCl_2$, 25 sorbitol, and 10 HEPES, adjusted to pH 7.2 with NaOH. The dorsal root ganglions were then digested with Liberase TM (0.35 U/ml; Roche Diagnostics) for 20 min, before another 15 min with Liberase TL (0.25 U/ml; Roche Diagnostics) and papain (30 U/ml, Worthington Biochemical) in complete saline solution containing 0.5 mM EDTA at 37°C. The dorsal root ganglion tissue was triturated with a fire-polished Pasteur pipette. Dispersed neurons were suspended in Dulbecco's modified Eagle medium containing 1 mg/ml bovine serum albumin and 1 mg/ml trypsin inhibitor (Sigma-Aldrich) and plated onto poly-D-lysine/laminin coated glass coverslips (BioCoat, BD Biosciences). The Dulbecco's modified Eagle medium contained equal amounts of Dulbecco's modified Eagle medium and F12 (Gibco) with 10% foetal calf serum (Sigma) and 1% penicillin and streptomycin (Invitrogen). The cells were incubated at 37°C and used within 24 h after plating.

Whole-cell patch clamp recordings from acutely cultured dorsal root ganglion neurons

Whole-cell recordings were made from MRGPRA3$^+$ and MRGPRD$^+$ dorsal root ganglion neurons identified by the fluorescence of GFP using epifluorescence microscopy (Olympus, Japan). Whole-cell current and voltage-clamp experiments were performed at room temperature (20–22°C) using a Multiclamp 700A amplifier with pClamp 9 software (Molecular Device), as described (Qu *et al.*, 2011, 2012). Signals were sampled at 10 kHz or 20 kHz and filtered at 2 kHz. The patch pipettes were pulled from borosilicate glass capillaries (Sutter Instrument; Novato) using a P97 micropipette puller (Sutter Instrument) and had a resistance of 3–4 MΩ and 1–2 MΩ for current- and voltage-clamp recordings, respectively. The series resistance was routinely compensated at 60–80%.

Resting membrane potential was recorded for each neuron under the current clamp mode after stabilization (within 3 min). A neuron was included only if the resting potential was more negative than −40 mV and the spike overshoot was >15 mV. Action potentials were evoked by a series of depolarizing current steps, each 500 ms duration, in increments of 50 pA up to 1 nA delivered through the recording electrode. The number of action potentials evoked by a suprathreshold stimulus was estimated by injecting a 500-ms depolarizing current of a magnitude at twice rheobase. Input resistance was obtained from the slope of a steady-state current-voltage plot in response to a series of hyperpolarizing currents steps from −200 to −50 pA. For current clamp recordings, the internal solution contained (in mM): 120 K^+-gluconate, 20 KCl, 1 $CaCl_2$, 2 $MgCl_2$, 11 EGTA, 10 HEPES-K^+, 2 MgATP, with pH adjusted to 7.2 using Tris-base and osmolarity adjusted to 290–300 mOsm with sucrose. The external solution contained the following (in mM): 145 NaCl, 3 KCl, 2 $MgCl_2$, 2 $CaCl_2$, 10 glucose, and 10 HEPES, pH adjusted to 7.4 with NaOH. The liquid junction potential of 11 mV was corrected.

Na^+ current recordings were started ~3 min after establishing whole-cell voltage-clamp configuration, as described (Fan *et al.*, 2011). The neurons with the ratio of peak tetrodotoxin (TTX)-resistant to TTX-sensitive currents <10% were excluded for analysis (Fan *et al.*, 2011). Linear leakage currents were digitally subtracted on-line using a P/4 procedure. The internal solution contained the following (in mM): 140 CsF, 10 NaCl, 2 $MgCl_2$, 0.1 $CaCl_2$, 1 EGTA, and 10 HEPES, pH adjusted to 7.2 with CsOH. The bath solution contained (in mM): 35 NaCl, 105 choline Cl, 1 $MgCl_2$, 1 $CaCl_2$, 0.1 $CdCl_2$, 20 tetraethylammonium Cl, 10 glucose, and 10 HEPES, pH adjusted at 7.4 with NaOH. The liquid junction potential for Na^+ current recordings was calculated to be 11.5 mV but was not corrected, as it was constant across experimental groups (Fan *et al.*, 2011).

Histology

Mice were deeply anaesthetized with ketamine and xylazine and perfused transcardically with 0.1 M PBS followed by 4% paraformaldehyde in PBS. L3, L4 and L5 dorsal root ganglions from control and CHS MRGPRA3$^+$ or MRGPRD$^+$ mice ($n = 3$ mice for each group) were collected and fixed in the same fixative for 4 h. Then the dorsal root ganglions were cryoprotected overnight in 0.1 M PBS containing 30% sucrose. Dorsal root ganglions were cryosectioned at 20 μm thickness and mounted on slides. The nucleus was stained with 4′,6-diamidino-2-phenylindole (2 μg/ml) (Sigma). Images were captured using a Nikon Eclipse Ti-S fluorescent microscope equipped with an Andorra Technology camera (Nikon Instruments Inc.) and analysed using Adobe Photoshop CS5 software. For quantitative analysis, at least one dorsal root ganglion was chosen from each mouse. A total of at least eight sections from each dorsal root ganglion were randomly selected. The proportions of MRGPRA3$^+$ or MRGPRD$^+$ neurons were calculated by the number of GFP-expressing neurons divided by the total number of neuronal profiles. Only the neurons with a clearly visible nucleus in the tissue section were counted.

Data analysis

Electrophysiological data were analysed using pClamp 9 software (Molecular Devices) and Origin 6.0 (OriginLab). For the analysis of voltage versus current relationships, the current density (pA/pF) was calculated by dividing the peak current by the cell capacitance. For the analysis of steady-state activation, Na^+ conductance (G) at each test pulse voltage (V) was calculated from the corresponding current (I) using the equation $G = I / (V - V_{rev})$, where V_{rev} is the reversal potential of Na^+ current which was determined for each cell individually. Activation curves were obtained by plotting normalized conductance (G / G_{max}) against test pulse voltage (V) and then fitting with Boltzmann functions in the forms of $G / G_{max} = 1 / \{1 + \exp [(V_{1/2, act} - V) / k]\}$, where G_{max} is the maximal Na^+ conductance, $V_{1/2, act}$ is the voltage for half-maximum activation and k is the slope factor. Steady-state inactivation was examined using a series of 500 ms prepulses from −130 to −10 mV with 10 mV increments, before a 30 ms test pulse of −10 mV (Fan *et al.*, 2011). The inactivation of TTX-resistant Na^+ currents was assumed to occur positive to −50 mV. Peak inward currents (I) obtained from steady-state inactivation protocol were normalized to the maximal peak current (I_{max}) and fitted with a negative Boltzmann function of the form: $I / I_{max} = 1 / \{1 + \exp[(V - V_{1/2, inact}) / k]\}$, where V represents the inactivation prepulse potential, $V_{1/2, inact}$ represents the voltage at which activation is half-maximal and k is the slope factor.

Means are presented with the standard error of the mean. Statistical analyses were performed using a student's *t*-test or one-way repeated measures analysis of variance with Bonferroni adjustments for pairwise comparisons or Tukey's *post hoc* test as appropriate. Comparisons of proportions were made using Fisher's exact test. Significance was set at $P < 0.05$.

Results

SADBE challenge induced contact hypersensitivity accompanied by itch and pain behaviour

SADBE challenge to the calf of sensitized mice induced progressive CHS characterized by skin swelling, consistent with previous findings with SADBE and other contact sensitizers (Christensen and Haase, 2012; Honda *et al.*, 2013). In comparison with pre-challenge values, the thickness of the calf skin was significantly increased after the second SADBE challenge ($n = 13$ mice) but not after the second application of the acetone vehicle ($n = 6$) (Fig. 1A, paired *t*-tests). In addition, SADBE challenge produced spontaneous biting and licking directed to the SADBE-treated calf skin of the mouse. In comparison with pre-challenge values, the cumulative durations of spontaneous biting and licking were each significantly greater after the first and the second SADBE challenge (Fig. 1B; repeated measures analysis of variance, Bonferroni adjustments for pairwise comparisons; $n = 20$). There were no significant differences in the cumulative duration of spontaneous biting and licking before versus after each application of acetone alone (Fig. 1B; $n = 6$).

To test further the validity of the use of biting versus licking on the calf as behavioural indicators of itch and pain, we used the 'cheek model' in which the behavioural indicators of itch and pain on the cheek were scratching the cheek with the hind limb versus wiping the cheek with the forelimb, respectively (Shimada and LaMotte, 2008). In comparison with pre-challenge values, there was a significantly greater number of bouts of site-directed scratching after each SADBE challenge to the cheek and a significantly greater number of site-directed wipes after the second SADBE challenge (Fig. 1C; repeated measures analysis of variance with Bonferroni adjustments, $n = 10$). In contrast, no such significant increases were observed after each application of acetone (Fig. 1C, $n = 6$). Together, these data support the validity of measuring itch and nociceptive behaviours in the mouse during the development of SADBE-induced CHS.

If MRGPRA3$^+$ neurons can mediate scratching behaviour evoked by pruritic chemicals (Han *et al.*, 2013), one would expect that ablation of these neurons might result in a decrease in spontaneous scratching accompanying CHS. We therefore induced CHS in MRGPRA3$^{GFP\text{-}Cre}$;ROSA26^{DTR} mice in which the MRGPRA3$^+$ neurons were selectively ablated and DTX-treated ROSA26^{DTR} control mice (Han *et al.*, 2013). When challenged with SADBE on the nape of the neck, the total number of bouts of site-directed scratching was significantly lower in the mice with the ablated MRGPRA3 neurons ($n = 7$) than in the control mice ($n = 8$, unpaired *t*-test; Fig. 1D).

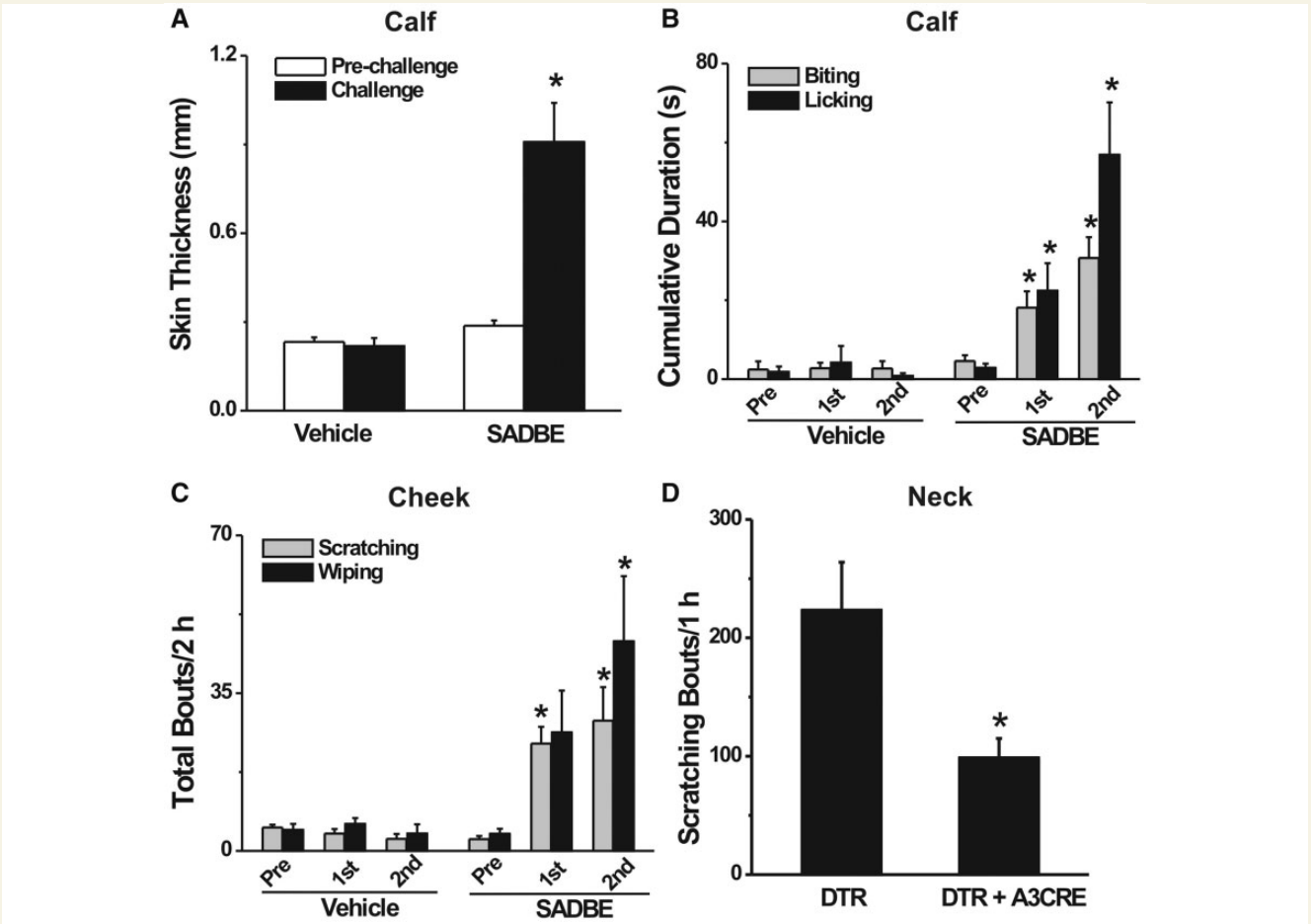

Figure 1 SADBE challenge induced CHS and spontaneous site-directed behaviours in previously sensitized mice. (**A**) In comparison with pre-challenge values, the thickness of calf skin was significantly increased 24 h after the second SADBE challenge ($n = 13$ mice) whereas applications of acetone alone (vehicle) had no significant effect ($n = 6$) (paired t-test). (**B**) After SADBE challenge of the calf, cumulative durations of spontaneous biting and licking of the calf were each significantly increased over pre-challenge (Pre) values ($n = 20$) but not after applications of acetone ($n = 6$) (repeated measures analysis of variance with Bonferroni adjustments). (**C**) After SADBE challenge of the cheek, the number of bouts of spontaneous scratching and wiping were each significantly increased over pre-challenge values ($n = 10$) whereas the acetone vehicle itself had no significant effect ($n = 6$) (repeated measures analysis of variance with Bonferroni adjustments). (**D**) SADBE challenge to the nape of the neck in previously sensitized mice evoked significantly fewer bouts of site-directed scratching in MRGPRA3$^{GFP\text{-}Cre}$;ROSA26^{DTR} mice with selective ablation of MRGPRA3$^+$ neurons ($n = 7$) than control ROSA26^{DTR} mice ($n = 8$) (unpaired t-test).*$P < 0.05$.

SADBE challenge produced spontaneous activity in a portion of cutaneous MRGPRA3$^+$ and MRGPRD$^+$ neurons *in vivo*

As MRGPRA3$^+$ and a subset of MRGPRD$^+$-expressing neurons were recently identified as two specific types of pruriceptive cutaneous dorsal root ganglion neurons, we next examined whether these putative itch-mediating dorsal root ganglion neurons became spontaneously active after SADBE challenge in a physiologically relevant setting with an *in vivo* recording method. Fourteen MRGPRA3$^+$ and 22 MRGPRD$^+$ neurons were recorded from CHS mice and 12 MRGPRA3$^+$ and 19 MRGPRD$^+$ -expressing neurons were recorded from control (acetone treated) mice. All the neurons tested were cutaneous C-nociceptive units with a peripheral receptive field within vehicle- or SADBE-treated skin area (Fig. 2). In control mice, both types of neurons were silent, i.e. exhibited no spontaneous activity, in agreement with previous studies (Liu *et al.*, 2012; Han *et al.*, 2013). All MRGPRA3$^+$ neurons tested responded to both noxious heat and mechanical stimuli, and thus were classified as C-mechanoheat (CMH) polymodal nociceptors. Less than half of the MRGPRD$^+$ neurons tested were CMH nociceptors, whereas the remaining neurons responded only to noxious mechanical stimulus and were classified as C-mechano (CM) nociceptors. In the animals with CHS, 6 of 14 (43%) MRGPRA3$^+$ neurons tested exhibited spontaneous activity in the absence of previous cutaneous stimulation (Fig. 2A–F). Moreover, 4 of 14 (29%) MRGPRA3$^+$ neurons from CHS mice displayed abnormal after-discharges in response to heat and to

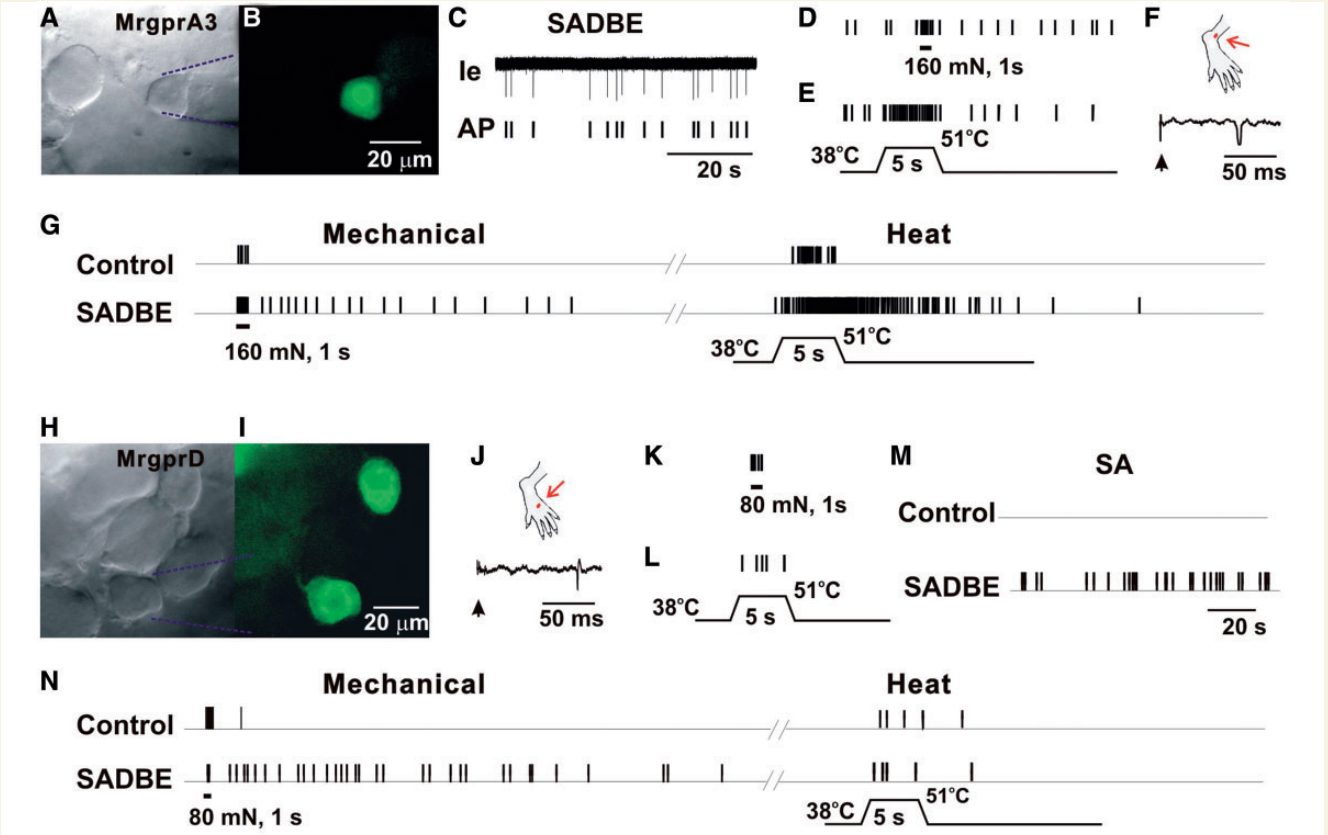

Figure 2 CHS produced spontaneous activity and enhanced stimulus-evoked responses in MRGPRA3$^+$ and MRGPRD$^+$ neurons. (**A**) Bright-field image of a neuron under recording with the extracellular electrode (outlined with dashed blue lines). (**B**) Fluorescent microscopy revealed the expression of GFP (i.e. MRGPRA3) in this neuron. (**C**) Original extracellular recording trace (Ie) and action potential markers (AP) indicated the presence of abnormal spontaneous activity (SA) of this neuron, without any external stimulation. (**D**) Responses of this MRGPRA3-GFP$^+$ neuron to 160 mN force through a 200 μm diameter probe (1 s). (**E**) Response to heat stimulation (38 to 51°C, 5 s), in the presence of ongoing spontaneous activity. (**F**) Location of cutaneous receptive field (red dot) of this neuron on the hairy skin of hind paw (the region challenged with SADBE), and conduction velocity (0.67 m/s, lower trace) obtained with electrical stimulation (arrow) to the peripheral receptive field. (**G**) Responses of the MRGPRA3$^+$ neuron innervating the vehicle control or SADBE-challenged skin to mechanical stimulus of 160 mN force through a 200 μm probe for 1 s, and to heat stimuli (38 to 51°C, 5 s). The neuron innervating SADBE-challenged skin was initially silent but showed prolonged after-discharge following the 160 mN mechanical stimulation and heating. No stimulus-evoked after-discharges were observed in MRGPRA3 neurons from control animals. (**H**) Bright-field image of a MRGPRD$^+$ neuron under recording with the extracellular electrode (outlined with dashed blue lines). (**I**) Fluorescent microscopy revealed the expression of GFP (or MRGPRD) in this neuron. (**J**) Location of cutaneous peripheral receptive field (red dot) of this neuron on the hairy skin of hind paw (the region challenged with SADBE), and conduction velocity (0.57 m/s, lower trace) obtained with electrical stimulation (arrow) to the peripheral receptive field. (**K** and **L**) Responses of MRGPRD-GFP$^+$ neuron to 80 mN force through a 200 μm diameter probe (1 s), and to heat stimulation (38 to 51°C, 5 s). This neuron did not exhibit spontaneous activity. (**M**) Spontaneous activity was observed in a subset of MRGPRD$^+$ neurons from CHS mice, but not from controls. (**N**) MRGPRD$^+$ neurons from CHS mice exhibited prolonged after-discharges in response to noxious mechanical stimulus (80 mN, 1 s) but not heat (38 to 51°C, 5 s). No prolonged after-discharges were evoked by noxious mechanical and heat stimuli in MRGPRD$^+$ neurons from control animals.

mechanical stimuli. In contrast, no after-discharges occurred in response to such stimuli in MRGPRA3$^+$ neurons from control mice (Fig. 2G). The proportion of MRGPRA3+ neurons with spontaneous activity and after-discharges was significantly increased in CHS mice (57%) as compared with control animals (0%) (Fisher's exact test). Only 1 of 22 MRGPRD$^+$ neurons recorded from CHS mice exhibited spontaneous activity (Fig. 2H–M). In addition, mechanically evoked after-discharges were observed in 3 (including the spontaneous activity neuron) of 22 MRGPRD$^+$ neurons from CHS mice, but not in any of the MRGPRD$^+$ neurons from control animals (Fig. 2N). No abnormal heat-evoked after-discharges occurred in MRGPRD$^+$ neurons from both control and CHS mice (Fig. 2N). There was no significant difference in the proportion of MRGPRD$^+$ neurons with abnormal activity between control (0%) and CHS mice (14%) (Fisher's exact test). Nevertheless, the presence of spontaneous activity in one neuron and abnormal mechanically evoked discharges in this and two others are consistent with the idea that the excitability of the peripheral terminals of a portion of the MRGPRD$^+$ neurons was increased after CHS.

As a test of whether CHS may have caused an upregulation in the expression of MRGPRA3$^+$ or MRGPRD$^+$ in other types or greater numbers of the same types of neurons, we measured, in individual dorsal root ganglions, the proportion of the total number of counted cells that expressed GFP (indicating expression of MRGPRA3 or MRGPRD). The proportions were averaged for the number of dorsal root ganglions sampled from mice serving as controls (acetone treated) versus mice that developed SADBE-induced CHS. Similar to previous studies (Liu *et al.*, 2008), the percentages of MRGPRA3$^+$ and MRGPRD$^+$ neurons from control mice were $4.4 \pm 0.3\%$ ($n = 3$ dorsal root ganglions) and $23.8 \pm 2.9\%$ ($n = 4$), respectively. In CHS mice, the percentages of MRGPRA3$^+$ and MRGPRD$^+$ neurons were $4.8 \pm 0.2\%$; ($n = 3$) and $24.6 \pm 1.8\%$ ($n = 3$), each of which was not significantly different from corresponding control values (Fisher's exact tests). Thus, there was no evidence for a change in the proportion of neurons expressing each type of MRGPRs after CHS.

SADBE challenge increased the excitability of dissociated MRGPRA3$^+$ and MRGPRD$^+$ neurons

To further investigate the excitability of cutaneous itch-mediating neurons, whole-cell recordings were made from acutely dissociated, fluorescently labelled MRGPRA3$^+$ and MRGPRD$^+$ neurons after the second challenge either with SADBE (CHS group) or acetone (control group) (Table 1 and Fig. 3). Because both types of neurons have been shown to innervate the skin, it was assumed that these neurons had innervated the chemically treated skin of the hind leg. For each type of neuron (MRGPRA3$^+$ and MRGPRD$^+$), the excitability was measured under current-clamp conditions and the mean values of each parameter were compared for CHS and control conditions using unpaired *t*-tests (Table 1). In comparison with controls, both MRGPRA3$^+$ and MRGPRD$^+$ neurons from CHS mice exhibited significantly more depolarized resting membrane potentials, lower rheobases, and increased numbers of action potentials evoked at twice rheobase (Table 1 and Fig. 3). In contrast, for either MRGPRA3$^+$ or MRGPRD$^+$ neurons, no significant differences were found in cell capacitance, input resistance, or action potential voltage threshold (Table 1).

SADBE challenge increased voltage-gated Na$^+$ currents

As no change was observed in the membrane input resistance of MRGPRA3$^+$ and MRGPRD$^+$ neurons from CHS mice, the increased excitability seemed likely to be a result of alterations in voltage-gated ion channels. The total Na$^+$ currents were generated by a series of test pulses, each 30 ms in duration, from -100 mV to $+50$ mV in 5-mV steps, preceded by a 500-ms prepulse to -100 mV (Fan *et al.*, 2011). In addition, we applied a prepulse inactivation protocol with a 500-ms step of -50 mV to isolate TTX-resistant Na$^+$ currents (Fig. 4A). The TTX-sensitive Na$^+$ current was obtained by digitally subtracting the TTX-resistant component from the total Na$^+$ current. As the properties of the TTX-sensitive (or TTX-resistant) Na$^+$ currents were similar for MRGPRA3$^+$ and MRGPRD$^+$ under control conditions and the effects of SADBE challenge in changing these currents were the same for each type of neuron, we combined the results for these two types of neurons for ease of presentation. The mean peak current density of the TTX-sensitive Na$^+$ currents was significantly greater for the CHS group ($n = 27$) compared with controls ($n = 24$) (Fig. 4; repeated measures analysis of variance and Tukey *post hoc* comparisons). Similarly, the TTX-resistant Na$^+$ peak current density was also increased significantly for CHS neurons ($n = 27$) compared to neurons from control animals (Fig. 4, $n = 24$).

We further tested whether an increase in Na$^+$ current density observed in the CHS group was because of significant changes in the voltage dependence of activation and inactivation of Na$^+$ currents. We found that the voltage-dependence of TTX-sensitive or TTX-resistant Na$^+$ currents was not significantly different between control and CHS groups (Fig. 5; unpaired *t*-tests). For TTX-sensitive Na$^+$ currents, the mean activation midpoint ($V_{1/2}$) from fitting the data with a Boltzmann function did not significantly differ for control and CHS (-28.0 ± 3.2 mV, $n = 8$, versus. -25.7 ± 0.3 mV, $n = 15$, respectively). Neither was there a significant difference in the mean slope factor for activation (control: 4.0 ± 0.8, $n = 8$; CHS: 4.7 ± 0.1, $n = 15$; Fig. 5A). Similarly, for TTX-resistant Na$^+$ currents, we also found no significant differences for control versus CHS groups in the mean $V_{1/2}$ (-16.3 ± 1.2 mV, $n = 13$, versus -15.6 ± 1.4 mV, $n = 14$, respectively) or in the mean slope factor for activation (4.7 ± 0.9,

Table 1 Membrane properties of MRGPRA3$^+$ and MRGPRD$^+$ neurons from control (vehicle-treated) and CHS (SADBE-challenged) mice

	MRGPRA3$^+$		MRGPRD$^+$	
	Control ($n = 12$)	SADBE ($n = 17$)	Control ($n = 12$)	SADBE ($n = 16$)
Cell capacitance (pF)	17.8 ± 1.7	14.8 ± 1.4	15.5 ± 1.3	14.1 ± 1.3
Resting membrane potential (mV)	-62.2 ± 1.0	-53.4 ± 3.2***	-61.3 ± 1.0	-53.7 ± 1.3**
Rheobase (pA)	102.5 ± 16.2	25.9 ± 5.9***	144.2 ± 37.7	49.3 ± 6.5*
Input resistance (MΩ)	560.3 ± 67.7	624.8 ± 64.1	651.0 ± 77.8	631.0 ± 75.8
Action potential voltage threshold (mV)	-23.7 ± 1.9	-23.6 ± 2.2	-26.8 ± 4.0	-18.7 ± 1.1
Number of action potentials at twice rheobase	1.4 ± 0.2	3.1 ± 0.6**	1.3 ± 0.2	4.6 ± 0.9**

Data are expressed as mean ± SEM. *$P < 0.05$; **$P < 0.01$; ***$P < 0.001$; as compared with control group, unpaired *t*-test.

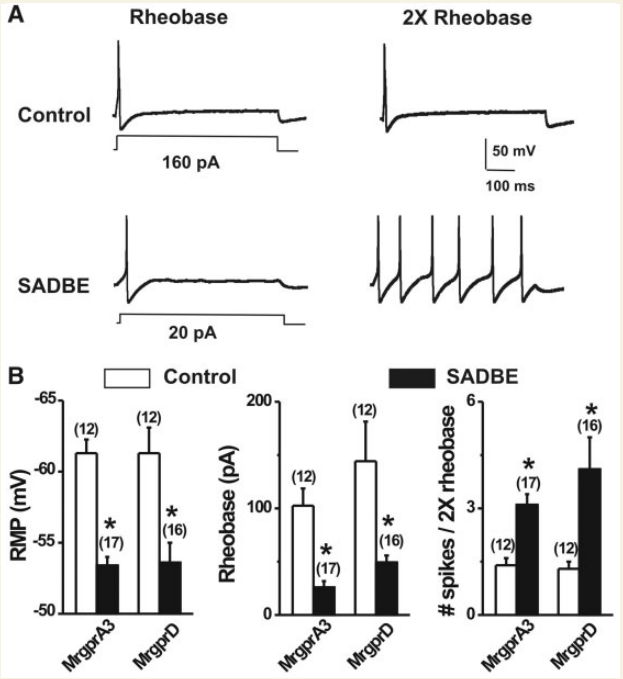

Figure 3 SADBE challenge increased the excitability of MRGPRA3$^+$ and MRGPRD$^+$ neurons. (**A**) Representative traces of action potentials elicited at rheobase and twice rheobase in MRGPRA3$^+$ neurons from vehicle control and SADBE-treated mice. SADBE challenge results in a reduction of rheobase while increasing the number of action potentials evoked by a 2 × rheobase current injection. (**B**) MRGPRA3$^+$ and MRGPRD$^+$ neurons from SADBE-challenged mice each exhibited a more depolarized resting membrane potential (RMP), lower mean rheobase, and greater number of action potentials at twice rheobase, as compared to control group. Cell numbers tested are indicated in the parentheses. $^*P < 0.05$ versus vehicle control, unpaired *t*-test.

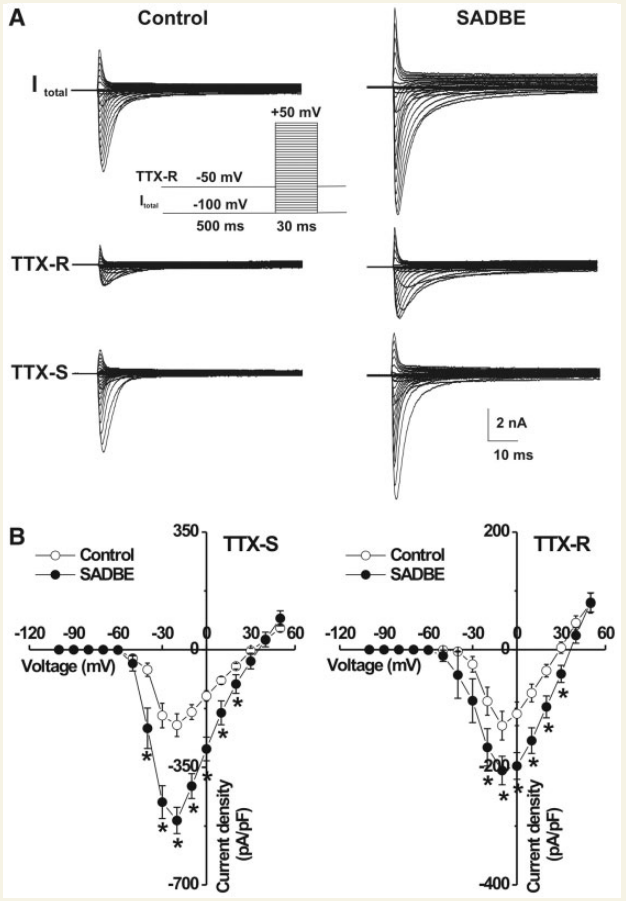

Figure 4 Voltage-gated Na$^+$ currents of MRGPR neurons were increased after the second SADBE challenge. (**A**) Representative traces of voltage-gated Na$^+$ currents in two MRGPRA3$^+$ neurons, one from an acetone-treated control mouse (*left*) and the other from a SADBE-treated mouse. Total Na$^+$ currents (I_{total}; *top*) were generated by stepwise 30-ms test pulses in 5-mV steps from −100 to +50 mV, preceded by a 500-ms prepulse of −100 mV (inset). TTX-resistant (TTX-R) currents (*middle*) were generated using the same series of test pulses but preceded by a 500-ms prepulse of −50 mV. TTX-sensitive (TTX-S) currents (*bottom*) were obtained by digitally subtracting TTX-resistant currents from total Na$^+$ currents. (**B**) The peak current densities of both TTX-sensitive (*left*) and TTX-resistant (*right*) Na$^+$ currents was significantly larger in SADBE-treated mice (closed circles, $n = 27$ neurons), as compared with controls (open circles, $n = 24$ neurons). Data for MRGPRA3$^+$ and MRGPRD$^+$ neurons were similar and thus combined (see main text). $^*P < 0.05$, SADBE versus vehicle control, one-way repeated measures analysis of variance with Tukey *post hoc* comparisons.

$n = 13$, versus 6.6 ± 0.8, $n = 14$, respectively; Fig. 5B). In addition, SADBE challenge did not significantly affect the voltage-dependence of steady-state inactivation of TTX-sensitive or TTX-resistant Na$^+$ currents as demonstrated by non-significant differences between control and CHS groups in mean values of either the $V_{1/2}$ or the slope factor for current inactivation for either TTX-sensitive or TTX-resistant Na$^+$ currents (Fig. 5 and data not shown).

Discussion

Peripheral afferent and neuronal hyperexcitability accompanying contact hypersensitivity

Although the pathogenesis of allergic contact dermatitis is widely studied, little is known of the effects of allergic contact dermatitis on the functional properties of pruriceptive cutaneous dorsal root ganglion neurons. The present study specifically focused on the spontaneous itch and pain behaviours and the changes in the excitability of cutaneous MRGPRA3$^+$ and MRGPRD$^+$ neurons after CHS, the murine model of allergic contact dermatitis in humans. These neurons, or a subset, have been implicated in the encoding of itch or pain (Cavanaugh *et al.*, 2009; Liu *et al.*, 2012; Han *et al.*, 2013). We provide several observations that support the presence of hyperexcitability of these neurons after CHS. First, *in vivo* electrophysiological recordings revealed spontaneous activity in a subpopulation of MRGPRA3$^+$ and

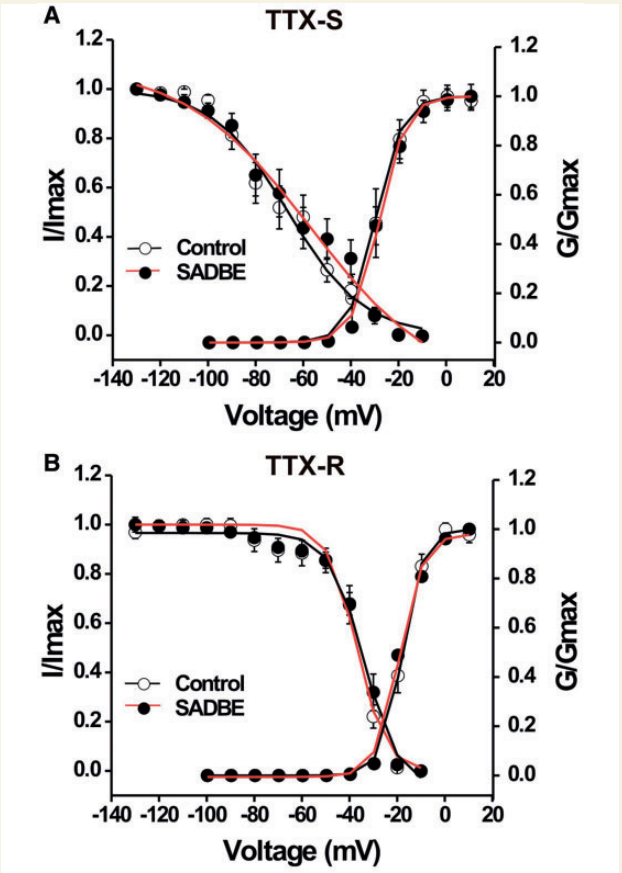

Figure 5 Comparison of voltage-dependent activation and steady-state inactivation curves of TTX-sensitive and TTX-resistant Na^+ currents in MRGPR neurons between vehicle-treated and SADBE-challenged mice. Data were pooled for MRGPRA3$^+$ and MRGPRD$^+$ neurons. (**A**) For activation curves, normalized conductance (G / Gmax) was plotted against test pulse voltage and fitted to a Boltzmann function. (**B**) For inactivation curves, normalized current (I / Imax) was plotted against prepulse voltage and fitted to a negative Boltzmann function. Line represents the average of the individual curve fits. There were no significant differences in the levels of activation or inactivation for TTX-sensitive (**A**) and TTX-resistant (**B**) currents between the neurons from control (open circles) and SADBE-treated mice (closed circles).

MRGPRD$^+$ neurons innervating SADBE-challenged skin, but not in neurons from control animals. Second, mechanical stimuli evoked abnormal after-discharges in a subset of MRGPRA3$^+$ and MRGPRD$^+$ neurons with receptive fields in SADBE-challenged skin. Also, some MRGPRA3$^+$ neurons from CHS mice exhibited prolonged after-discharges when noxious heat was applied to their receptive fields. Whether these abnormal discharges or possible changes in response thresholds (not presently measured) are associated with an increase in stimulus evoked itch or pain behaviour in the mouse analogous to enhanced stimulus evoked pain and itch in humans (Sikand *et al.*, 2012) awaits further experimentation.

The dissociated cell bodies of MRGPRA3$^+$ and MRGPRD$^+$ neurons became hyperexcitable after CHS, as indicated by a depolarized resting membrane potential, a significant decrease in rheobase and an increase in the number of action potential discharges evoked at twice rheobase. An increase in the excitability of the cell bodies of MRGPRA3$^+$ neurons from SADBE-treated mice may be linked to the hyperexcitability of their peripheral terminals, which might account for the after-discharges observed when their nerve terminals were stimulated by noxious heat and mechanical stimuli.

Although the cell bodies of MRGPRD$^+$ neurons exhibited signs of enhanced excitability, their peripheral terminals were less likely to exhibit signs of hyperexcitability than those of the MRGPRA3$^+$ neurons as a result of CHS. No after-discharges were observed in MRGPRD$^+$ neurons when noxious heat was delivered to their peripheral receptive fields. And, only a small proportion of MRGPRD$^+$ neurons from CHS mice exhibited spontaneous activity or abnormal after-discharges in response to mechanical force compared to MRGPRA3$^+$ neurons. One possible reason for these differences at the peripheral terminals is that, in contrast to MRGPRD$^+$ neurons, MRGPRA3$^+$ neurons express TRPV1 and respond to more types of pruritic and algesic chemical stimuli (Liu *et al.*, 2012; Han *et al.*, 2013) thereby possibly making them more responsive to endogenous inflammatory and other chemical mediators after the development of CHS. In the future it will be interesting to test the responses of both types of neurons to chemical pruritogens that, for human subjects with SADBE-induced allergic contact dermatitis elicited enhanced itch sensations (Sikand *et al.*, 2012).

Mechanisms of the hyperexcitability of MRGPRA3$^+$ and MRGPRD$^+$ neurons

Our findings demonstrated that CHS produced a significant increase in the magnitude of TTX-sensitive and TTX-resistant Na^+ currents but without any changes in the kinetics of activation and inactivation, which may underlie neuronal hyperexcitability observed in cutaneous MRGPRA3$^+$ and MRGPRD$^+$ neurons from CHS mice. Changes in these currents have been proposed to underlie the increased neuronal excitability found in other studies of peripheral inflammation. Peripheral inflammation of skin produced by an injection of carrageenan (Tanaka *et al.*, 1998) or complete Freund's adjunct (Gould *et al.*, 2004) caused an increase in both TTX-sensitive and TTX-resistant Na^+ currents without affecting the kinetics of activation or inactivation in small-diameter dorsal root ganglion neurons. Unlike our model of allergic contact dermatitis in humans, these models of inflammatory pain are toxic and cannot be used in humans. The mechanisms whereby peripheral inflammation modulates voltage-gated Na^+ channels require further investigation. The inflammatory milieu surrounding the nerve terminals in the skin contains numerous inflammatory mediators during CHS (Kondo *et al.*, 1994; Westphal *et al.*, 2003; Christensen and Haase, 2012), such as tumor necrosis factor alpha (TNFα) and interleukin-1β (IL-1β), which may be retrogradely transported to cell bodies of dorsal root ganglion neurons and contribute to the increased Na^+ currents observed in this study. Indeed, TNFα and (IL-1β) have been demonstrated to augment TTX-sensitive and TTX-resistant Na^+

currents in nociceptive dorsal root ganglion neurons (Binshtok *et al.*, 2008; Czeschik *et al.*, 2008). Although an increase in Na^+ currents likely contributes to the lower rheobase observed in the present study, we cannot exclude a role for other ion channels. As no significant changes in input resistance of dorsal root ganglion neurons were observed after CHS, it is unlikely that leak channels account for neuronal hyperexcitability in the murine model of allergic contact dermatitis.

Implications for itch and pain associated with allergic contact dermatitis

Itch and pain often accompany skin diseases, such as allergic contact dermatitis and atopic dermatitis. Although the immune mechanisms of CHS have been extensively explored in murine models of allergic contact dermatitis (Christensen and Haase, 2012; Honda *et al.*, 2013), less is known of the itch and pain behaviours and their underlying neural mechanisms. Behavioural assays of itch have typically used a single response indicator such as scratching the site of chemical application to the ear or nape of the neck (Liu *et al.*, 2013). By applying SADBE to the cheek or to the calf of the hindlimb, i.e. locations that allow the opportunity for distinguishing itch- and pain-like site-directed behaviours (Shimada and LaMotte, 2008; Akiyama *et al.*, 2010*a*; LaMotte *et al.*, 2011), we found that both types of behaviour were evoked during the elicitation phase of CHS. Analogously, sensations of itch and nociceptive sensations were reported when SADBE was applied to the skin of previously sensitized human subjects (Sikand *et al.*, 2012). Moreover, SADBE-treated human skin exhibited alloknesis, hyperknesis, and hyperalgesia to mechanical stimuli, itch sensation to noxious heat and an enhanced itch to intradermal injection of histamine, BAM8-22 (ligand for MRGPRC11 in mice and MRGPRX1 in humans), or beta-alanine (MRGPRD ligand in both humans and mice) (Sikand *et al.*, 2012). In humans, MRGPRX1 shares homology with murine MRGPRA3 and MRGPRC11. Thus, it is possible that peripheral pruriceptive neurons expressing MRGPRD or MRGPRX1 may become more excitable after experimental allergic contact dermatitis in humans. $MRGPRA3^+$ and $MRGPRD^+$ neurons were recently identified as candidates for mediating acute itch in mice evoked by pruritic chemicals that also evoke itch and nociceptive sensations in humans (Liu *et al.*, 2012; Han *et al.*, 2013). $MRGPRA3^+$ neurons play a critical role in histamine-dependent acute itch (Han *et al.*, 2013) whereas subpopulations of $MRGPRD^+$ neurons mediate the histamine-independent itch elicited by beta-alanine (Liu *et al.*, 2012) and mechanically evoked pain behaviour (Cavanaugh *et al.*, 2009) in mice under normal conditions. Also, $MRGPRA3^+$ neurons were recently shown to be involved in dry skin chronic itch and allergic itch (Han *et al.*, 2013).

Our findings indicate the possibility that the enhanced excitability of $MRGPRA3^+$ and $MRGPRD^+$ neurons may contribute to the itch and pain associated with CHS and the accompanied dysaesthesias. First, ablation of $MRGPRA3^+$ neurons significantly reduced the spontaneous scratching on the nape of the neck of CHS mice. Although the behavioural responses of scratching the nape of neck may also indicate pain in addition to itch sensation, we consider that $MRGPRA3^+$ neurons contribute to CHS-induced itch rather than pain as $MRGPRA3^+$ neurons were specifically linked to itch but not pain regardless of the type of stimulus that activates the neuron (Han *et al.*, 2013). MRGPRD knockout mice would be useful in future studies of the role of MRGPRD in inflammatory itch and pain. Second, cutaneous $MRGPRA3^+$ neurons innervating SADBE-treated skin exhibited spontaneous firing, which might indicate a chronic sensitization of pruriceptive primary afferent fibres and itch-signalling superficial dorsal horn neurons and, as a consequence, lead to chronic hyperknesis and alloknesis. Spontaneously ongoing activity in C-pruriceptors was also identified in patients with chronic itch (Ikoma *et al.*, 2004). Indeed, peripheral sensitization of pruriceptive primary sensory afferents has been suggested as a mechanism underlying the chronic itch of atopic dermatitis (Schmelz *et al.*, 2003). Third, noxious heat and mechanical stimuli evoked abnormal after-discharges at peripheral terminals of $MRGPRA3^+$ neurons after CHS, suggesting that this subset of peripheral pruriceptors is potentially sensitized by CHS and exhibits increased sensitivity to certain cutaneous stimuli. The increased mechanosensitivity (i.e. the after-discharges) observed at the peripheral terminals of $MRGPRA3^+$ neurons may contribute to increased mechanically evoked itch (hyperknesis and alloknesis) that humans experience after SADBE (Sikand *et al.*, 2012). Enhanced responses of peripheral pruriceptors to pruritic chemicals have also been found in a rodent model of itch from dry skin (Akiyama *et al.*, 2010*b*). Further studies are required to determine whether $MRGPRA3^+$ and $MRGPRD^+$ neurons exhibit enhanced responses to pruritic chemical stimuli after CHS.

$MRGPRD^+$ neurons from CHS mice exhibited prolonged after-discharges in response to mechanical, but not heat stimulation of their receptive fields. Mechanical- and mechanoheat-sensitive $MRGPRD^+$ neurons may encode pain and itch, respectively (Liu *et al.*, 2012). Our *in vitro* study did not distinguish between $MRGPRD^+$ neurons that are responsive to noxious heat and beta-alanine and are thought to be pruriceptive (Liu *et al.*, 2012) and other $MRGPRD^+$ neurons that only respond to noxious mechanical stimuli. Perhaps the latter contributes to mechanical nociception, which was found to be impaired after ablation of MRGPRD neurons (Cavanaugh *et al.*, 2009). Thus, the sensitization of $MRGPRD^+$ neurons might in part contribute to pain behaviour observed in CHS. Although itch can be transiently relieved by scratching, the itch–scratch cycle can further exacerbate the inflammation and damage the skin, probably activating mechanosensitive nociceptors thereby increasing pain as well as itch (Takaoka *et al.*, 2007; Hashimoto *et al.*, 2011).

We used GFP markers for MRGPRA3 and MRGPRD to identify the cell bodies of same subset of neurons *in vivo* (functional studies in the intact neuron) and *in vitro* (mechanistic studies after acute dissociation). We did not investigate a possible role of the MRGPRA3 or MRGPRD receptors in SADBE-induced itch versus pain behaviour. Our findings do not allow us to speculate on the role of other receptors or other types of sensory neurons in these behaviours. For example, there is evidence that TRPA1-expessing neurons are critically involved in a murine model of CHS produced by repeated delivery of the contact allergen, oxazolone (Liu *et al.*, 2013). Nonetheless, our results have identified neuronal targets and ionic mechanisms of neuronal

hyperexcitability that might contribute to spontaneous itch and pain sensations and the related dysaesthesias associated with CHS. These neurons and the associated mechanisms of enhanced excitability could be targeted by new therapeutic strategies designed to treat the pain and itch from inflammatory diseases of the skin and other pruritic disorders as well.

Acknowledgements

We thank Pu Zhang, Yumei Li for genotyping of transgenic animals

Funding

This work was supported by NIH grants NS047399 and NS014624 (RHL); GM087369 and NS054791 (XD); National Science Foundation of China #81271239 (CM) and PUMC/CAMS/IBMS Funding #2011RC01 (CM). L. Qu is the recipient of a fellowship from the Canadian Institutes of Health Research (CIHR). K Fu is a recipient of a scholarship from Jinan University, China.

References

Akiyama T, Carstens MI, Carstens E. Differential itch- and pain-related behavioral responses and micro-opoid modulation in mice. Acta Derm Venereol 2010a; 90: 575–81.

Akiyama T, Carstens MI, Carstens E. Enhanced scratching evoked by PAR-2 agonist and 5-HT but not histamine in a mouse model of chronic dry skin itch. Pain 2010b; 151: 378–83.

Binshtok AM, Wang H, Zimmermann K, Amaya F, Vardeh D, Shi L, et al. Nociceptors are interleukin-1beta sensors. J Neurosci 2008; 28: 14062–73.

Camouse MM, Swick AR, Ryan CA, Hulette B, Gerberick F, Tinkle SS, et al. Determination of in vivo dose response and allergen-specific T cells in subjects contact-sensitized to squaric acid dibutyl ester. Dermatitis 2008; 19: 95–9.

Cavanaugh DJ, Lee H, Lo L, Shields SD, Zylka MJ, Basbaum AI, et al. Distinct subsets of unmyelinated primary sensory fibers mediate behavioral responses to noxious thermal and mechanical stimuli. Proc Natl Acad Sci USA 2009; 106: 9075–80.

Chen SC. Pruritus. Dermatol Clin 2012; 30: 309–21, ix.

Christensen AD, Haase C. Immunological mechanisms of contact hypersensitivity in mice. APMIS 2012; 120: 1–27.

Czeschik JC, Hagenacker T, Schafers M, Busselberg D. TNF-alpha differentially modulates ion channels of nociceptive neurons. Neurosci Lett 2008; 434: 293–8.

Fan N, Donnelly DF, LaMotte RH. Chronic compression of mouse dorsal root ganglion alters voltage-gated sodium and potassium currents in medium-sized dorsal root ganglion neurons. J Neurophysiol 2011; 106: 3067–72.

Fan N, Qu L, Ma C, Shimada SG, Zhang P, Han L, et al. Allergic contact dermatitis induces both itch behavior and hyperexcitability in a subpopulation of cutaneous dorsal root ganglion neurons in the mouse. New Orleans LA: Society for Neuroscience; 2012. Abstract Program No. 675.08.

Gould HJ III, England JD, Soignier RD, Nolan P, Minor LD, Liu ZP, et al. Ibuprofen blocks changes in Na v 1.7 and 1.8 sodium channels associated with complete Freund's adjuvant-induced inflammation in rat. J Pain 2004; 5: 270–80.

Han L, Ma C, Liu Q, Weng HJ, Cui Y, Tang Z, et al. A subpopulation of nociceptors specifically linked to itch. Nat Neurosci 2013; 16: 174–82.

Hashimoto Y, Takaoka A, Sugimoto M, Honma Y, Sakurai T, Futaki N, et al. Itch-associated scratching contributes to the development of dermatitis and hyperimmunoglobulinaemia E in NC/Nga mice. Exp Dermatol 2011; 20: 820–5.

Honda T, Egawa G, Grabbe S, Kabashima K. Update of immune events in the murine contact hypersensitivity model: toward the understanding of allergic contact dermatitis. J Invest Dermatol 2013; 133: 303–15.

Ikoma A, Fartasch M, Heyer G, Miyachi Y, Handwerker H, Schmelz M. Painful stimuli evoke itch in patients with chronic pruritus: central sensitization for itch. Neurology 2004; 62: 212–7.

Johanek LM, Meyer RA, Friedman RM, Greenquist KW, Shim B, Borzan J, et al. A role for polymodal C-fiber afferents in nonhistaminergic itch. J Neurosci 2008; 28: 7659–69.

Kini SP, DeLong LK, Veledar E, McKenzie-Brown AM, Schaufele M, Chen SC. The impact of pruritus on quality of life: the skin equivalent of pain. Arch Dermatol 2011; 147: 1153–6.

Kondo S, Pastore S, Shivji GM, McKenzie RC, Sauder DN. Characterization of epidermal cytokine profiles in sensitization and elicitation phases of allergic contact dermatitis as well as irritant contact dermatitis in mouse skin. Lymphokine Cytokine Res 1994; 13: 367–75.

LaMotte RH, Shimada SG, Sikand P. Mouse models of acute, chemical itch and pain in humans. Exp Dermatol 2011; 20: 778–82.

Liu B, Escalera J, Balakrishna S, Fan L, Caceres AI, Robinson E, et al. TRPA1 controls inflammation and pruritogen responses in allergic contact dermatitis. FASEB J 2013; 27: 3549–63.

Liu Q, Sikand P, Ma C, Tang Z, Han L, Li Z, et al. Mechanisms of itch evoked by beta-alanine. J Neurosci 2012; 32: 14532–7.

Liu Q, Tang Z, Surdenikova L, Kim S, Patel KN, Kim A, et al. Sensory neuron-specific GPCR Mrgprs are itch receptors mediating chloroquine-induced pruritus. Cell 2009; 139: 1353–65.

Liu Y, Yang FC, Okuda T, Dong X, Zylka MJ, Chen CL, et al. Mechanisms of compartmentalized expression of Mrg class G-protein-coupled sensory receptors. J Neurosci 2008; 28: 125–32.

Ma C, Donnelly DF, LaMotte RH. *In vivo* visualization and functional characterization of primary somatic neurons. J Neurosci Methods 2010; 191: 60–5.

Ma C, LaMotte RH. Multiple sites for generation of ectopic spontaneous activity in neurons of the chronically compressed dorsal root ganglion. J Neurosci 2007; 27: 14059–68.

Ma C, Nie H, Gu Q, Sikand P, Lamotte RH. *In vivo* responses of cutaneous C-mechanosensitive neurons in mouse to punctate chemical stimuli that elicit itch and nociceptive sensations in humans. J Neurophysiol 2012; 107: 357–63.

Qu L, Li Y, Pan X, Zhang P, LaMotte RH, Ma C. Transient receptor potential canonical 3 (TRPC3) is required for IgG immune complex-induced excitation of the rat dorsal root ganglion neurons. J Neurosci 2012; 32: 9554–62.

Qu L, Zhang P, LaMotte RH, Ma C. Neuronal Fc-gamma receptor I mediated excitatory effects of IgG immune complex on rat dorsal root ganglion neurons. Brain Behav Immun 2011; 25: 1399–407.

Ringkamp M, Schepers RJ, Shimada SG, Johanek LM, Hartke TV, Borzan J, et al. A role for nociceptive, myelinated nerve fibers in itch sensation. J Neurosci 2011; 31: 14841–9.

Schmelz M, Hilliges M, Schmidt R, Orstavik K, Vahlquist C, Weidner C, et al. Active "itch fibers" in chronic pruritus. Neurology 2003; 61: 564–6.

Scott AE, Kashon ML, Yucesoy B, Luster MI, Tinkle SS. Insights into the quantitative relationship between sensitization and challenge for allergic contact dermatitis reactions. Toxicol Appl Pharmacol 2002; 183: 66–70.

Shimada SG, LaMotte RH. Behavioral differentiation between itch and pain in mouse. Pain 2008; 139: 681–7.

Shinohara T, Harada M, Ogi K, Maruyama M, Fujii R, Tanaka H, et al. Identification of a G protein-coupled receptor specifically responsive to beta-alanine. J Biol Chem 2004; 279: 23559–64.

Sikand P, King BA, LaMotte RH. Psychophysical measurements of itch and nociceptive sensations in an experimental model of allergic

dermatitis in humans. New Orleans LA: Society for Neuroscience; 2012. Abstract Program No. 675.07.

Takaoka A, Arai I, Sugimoto M, Futaki N, Sakurai T, Honma Y, et al. Role of scratch-induced cutaneous prostaglandin D production on atopic-like scratching behaviour in mice. Exp Dermatol 2007; 16: 331–9.

Tanaka M, Cummins TR, Ishikawa K, Dib-Hajj SD, Black JA, Waxman SG. SNS Na+ channel expression increases in dorsal root ganglion neurons in the carrageenan inflammatory pain model. Neuroreport 1998; 9: 967–72.

Westphal GA, Schnuch A, Moessner R, Konig IR, Kranke B, Hallier E, et al. Cytokine gene polymorphisms in allergic contact dermatitis. Contact Dermatitis 2003; 48: 93–8.

Zylka MJ, Rice FL, Anderson DJ. Topographically distinct epidermal nociceptive circuits revealed by axonal tracers targeted to Mrgprd. Neuron 2005; 45: 17–25.